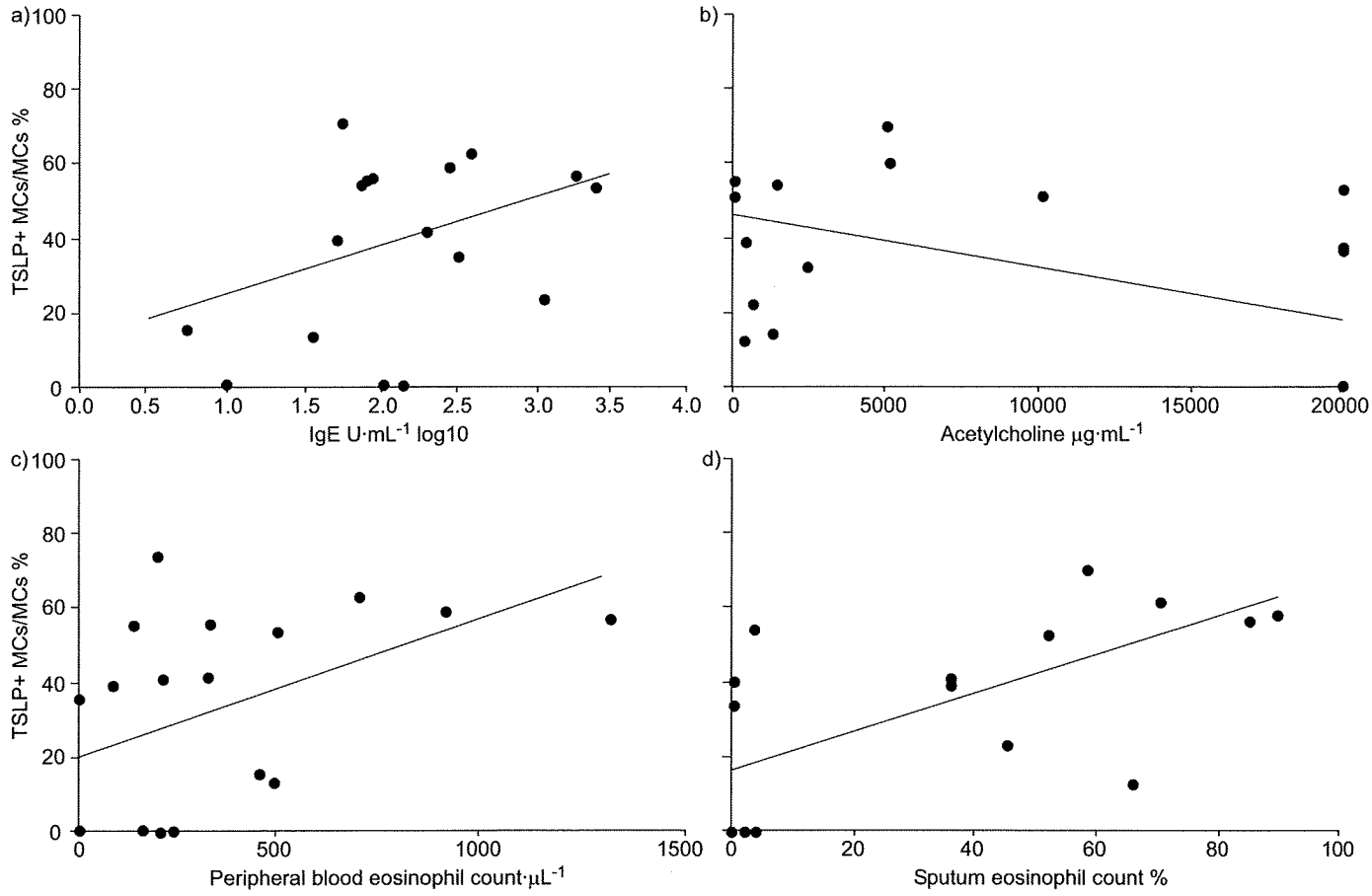

FIGURE 6. Correlation between the percentage of thymic stromal lymphopoietin (TSLP)+ mast cells (MCs) in the total population of MCs and various markers of bronchial asthma. Correlation between the percentage of TSLP+ MCs in the total population of MCs and: a) the serum immunoglobulin (Ig)E levels (asthma n=15, control n=4; r^2=0.131, p=0.048); b) the degree of bronchial hyperresponsiveness (asthma n=14, control n=9; r^2=0.252, p=0.024); c) the peripheral blood eosinophil count (asthma n=16, control n=8; r^2=0.243, p=0.045); and d) the sputum eosinophil count in asthmatic patients and healthy controls (asthma n=13, control n=8; r^2=0.437, p=0.024).

TSLP protein+ cells were MCs. This discrepancy may be due to the difference in the expression level between TSLP mRNA and TSLP protein. MCs are known to store cytokines in their cytoplasm. The level of TSLP in epithelial cells is synergistically increased by a combination of IL-4 and double-stranded RNA, suggesting that respiratory viral infection and the recruitment of Th2 cytokine-producing cells may amplify Th2 cytokine-mediated inflammation *via* the induction of TSLP in the airways of asthmatic subjects [9]. However, no evidence has been accumulated suggesting that allergens might directly induce TSLP production in the airways of asthmatics. Our *in vivo* and *in vitro* studies suggest that MCs are one of the main sources of TSLP in bronchial asthma; this is highly relevant to our understanding of allergic asthma. TSLP, which is released by MCs following aggregation of FcεRI, is capable of triggering DC-mediated Th2 inflammatory responses by induction of Th2-attracting chemokines, such as CCL17 and CCL22 [5], and by priming naïve Th2 cells to produce IL-4, IL-5, IL-13 and TNF-α, but not IL-10 [4, 5]. MC-derived TSLP plays an important role in the pathogenesis of bronchial asthma by facilitating cross-talk with DCs. It has been reported that TSLP stimulates the production of Th2 cytokines by human MCs synergistically with IL-1 and TNF-α [20], suggesting an autocrine/paracrine effect of MC-derived TSLP. Therefore, MC-derived TSLP in bronchial asthma may induce and aggravate allergic inflammation.

SUPPORT STATEMENT

The present study was supported in part by the Grants-In-Aid for Scientific Research (C) programme of the Ministry of Education, Culture, Sports, Science and Technology of the Japanese Government (project No. 18604009 and 20591195, to Y. Okayama), the Nihon University Joint Research Grant for 2008 (to Y. Okayama), the National Institute of Biomedical Innovation (project ID05-24,l to H. Saito and Y. Okayama), and the Matching Fund Subsidy for Private Universities from the Ministry of Education, Culture, Sports, Science and Technology of the Japanese Government (to C. Ra).

STATEMENT OF INTEREST

None declared.

ACKNOWLEDGEMENTS

We would like to thank T. Okada of Dokkyo Medical University School of Medicine (Tochigi, Japan) for his excellent technical assistance.

REFERENCES

1 Busse WW, Lemanske RF Jr. Asthma. *N Engl J Med* 2001; 344: 350–362.
2 Kay AB. The role of T lymphocytes in asthma. *Chem Immunol Allergy* 2006; 91: 59–75.
3 Leonard WJ. TSLP: finally in the limelight. *Nat Immunol* 2002; 3: 605–607.
4 Liu YJ. Thymic stromal lymphopoietin: master switch for allergic inflammation. *J Exp Med* 2006; 203: 269–273.
5 Soumelis V, Reche PA, Kanzler H, *et al.* Human epithelial cells trigger dendritic cell mediated allergic inflammation by producing TSLP. *Nat Immunol* 2002; 3: 673–680.
6 Zhou B, Comeau MR, De Smedt T, *et al.* Thymic stromal lymphopoietin as a key initiator of allergic airway inflammation in mice. *Nat Immunol* 2005; 6: 1047–1053.
7 Al-Shami A, Spolski R, Kelly J, *et al.* A role for TSLP in the development of inflammation in an asthma model. *J Exp Med* 2005; 202: 829–839.
8 Ying S, O'Connor B, Ratoff J, *et al.* Thymic stromal lymphopoietin expression is increased in asthmatic airways and correlates with expression of Th2-attracting chemokines and disease severity. *J Immunol* 2005; 174: 8183–8190.
9 Kato A, Favoreto S Jr, Avila PC, *et al.* TLR3- and Th2 cytokine-dependent production of thymic stromal lymphopoietin in human airway epithelial cells. *J Immunol* 2007; 179: 1080–1087.
10 Ito T, Wang YH, Duramad O, *et al.* TSLP-activated dendritic cells induce an inflammatory T helper type 2 cell response through OX40 ligand. *J Exp Med* 2005; 202: 1213–1223.
11 Wang YH, Ito T, Wang YH, *et al.* Maintenance and polarization of human th2 central memory T cells by thymic stromal lymphopoietin-activated dendritic cells. *Immunity* 2006; 24: 827–838.
12 Galli SJ, Nakae S, Tsai M. Mast cells in the development of adaptive immune responses. *Nat Immunol* 2005; 6: 135–142.
13 Gilfillan AM, Tkaczyk C. Integrated signalling pathways for mast-cell activation. *Nat Rev Immunol* 2006; 6: 218–230.
14 Okumura S, Kashiwakura J, Tomita H, *et al.* Identification of specific gene expression profiles in human mast cells mediated by Toll-like receptor 4 and FceRI. *Blood* 2003; 102: 2547–2554.
15 McCurdy JD, Olynych TJ, Maher LH, *et al.* Cutting edge: distinct toll-like receptor 2 activators selectively induce different classes of mediator production from human mast cells. *J Immunol* 2003; 170: 1625–1629.
16 Kulka M, Alexopoulou L, Flavell RA, *et al.* Activation of mast cells by double-stranded RNA: evidence for activation through Toll-like receptor 3. *J Allergy Clin Immunol* 2004; 114: 174–182.
17 Okumura S, Sagara H, Fukuda T, *et al.* FcεRI-mediated amphiregulin production by human mast cells increases mucin gene expression in epithelial cells. *J Allergy Clin Immunol* 2005; 115: 272–279.
18 Livak KJ, Schmittgen TD. Analysis of relative gene expression data using real-time quantitative PCR and the $2^{-\Delta\Delta CT}$ method. *Methods* 2001; 25: 402–408.
19 Makino S, Furusho K, Ohta K, *et al.* A survey on awareness and utilization of new asthma management guidelines in Japan. *J Asthma* 2003; 40: 701–708.
20 Allakhverdi Z, Comeau MR, Jessup HK, *et al.* Thymic stromal lymphopoietin is released by human epithelial cells in response to microbes, trauma, or inflammation and potently activates mast cells. *J Exp Med* 2007; 204: 253–258.
21 Zhao W, Oskeritzian CA, Pozez AL, *et al.* Cytokine production by skin-derived mast cells: endogenous proteases are responsible for degradation of cytokines. *J Immunol* 2005; 175: 2635–2642.
22 Tachimoto H, Ebisawa M, Hasegawa T, *et al.* Reciprocal regulation of cultured human mast cell cytokine production by IL-4 and IFN-γ. *J Allergy Clin Immunol* 2000; 106: 141–149.
23 Lorentz A, Wilke M, Sellge G, *et al.* IL-4-induced priming of human intestinal mast cells for enhanced survival and Th2 cytokine generation is reversible and associated with increased activity of ERK1/2 and c-Fos. *J Immunol* 2005; 174: 6751–6756.
24 Lora JM, Al-Garawi A, Pickard MD, *et al.* FcεRI-dependent gene expression in human mast cells is differentially controlled by T helper type 2 cytokines. *J Allergy Clin Immunol* 2003; 112: 1119–1126.
25 Toru H, Ra C, Nonoyama S, *et al.* Induction of the high-affinity IgE receptor (FcεRI) on human mast cells by IL-4. *Int Immunol* 1996; 8: 1367–1373.

Journal of General Virology (2010), **91**, 421–429 DOI 10.1099/vir.0.014258-0

Characterization of a rare natural intertypic type 2/type 3 penta-recombinant vaccine-derived poliovirus isolated from a child with acute flaccid paralysis

Yong Zhang,[1]† Haiyan Wang,[2]† Shuangli Zhu,[1] Yan Li,[2] Lizhi Song,[2] Yao Liu,[2] Guifang Liu,[2] Yorihiro Nishimura,[3] Li Chen,[1] Dongmei Yan,[1] Dongyan Wang,[1] Hongqiu An,[1] Hiroyuki Shimizu,[3] Aiqiang Xu[2] and Wenbo Xu[1]

Correspondence
Wenbo Xu
wenbo_xu1@yahoo.com.cn

[1]WHO WPRO Regional Polio Reference Laboratory and State Key Laboratory for Molecular Virology & Genetic Engineering, Institute for Viral Disease Control and Prevention, Chinese Center for Disease Control and Prevention, No. 27 Nanwei Road, Xuanwu District, Beijing 100050, PR China

[2]Shandong Center for Disease Control and Prevention, No. 27 Jingshi Road, Jinan 250014, PR China

[3]Department of Virology II, National Institute of Infectious Diseases, Tokyo 208-0011, Japan

A type 2 vaccine-derived poliovirus (VDPV) (strain CHN1025), with a 1.1 % (10/903) difference from Sabin strain in the *VP1* coding region, was isolated from a child with poliomyelitis caused by a poliovirus variant infection. The patient was from Shandong Province of China and developed acute flaccid paralysis in 1997. The child was infected with a rare and complicated penta-recombinant poliovirus with the uncommon genomic recombinant organization S2/S3/S1/S3/S1/S3. At least five successive rounds of recombination occurred in the *VP1* capsid coding region and in the *2C*, *3C* (twice) and $3D^{pol}$ non-capsid coding regions, respectively, during virus evolution. Strain CHN1025 had most of the characteristics of the type 2 vaccine strain; it had Sabin-specific epitopes, suggesting that the virus was antigenically indistinguishable from the Sabin 2 reference strain. Typical mutations in the 5′-untranslated region and VP1 associated with reversion to neurovirulence for Sabin 2 poliovirus were found, and the virus showed moderate neurovirulence in transgenic mice. A few nucleotide substitutions were located in the donor sequences, and two donor sequences contained no nucleotide substitutions, suggesting that these sequences were relatively new. The appearance of these mutations within approximately 192 days of at least five successive rounds of recombination events derived from a single ancestral infection illustrates the rapid emergence of new recombinants among VDPVs. This is the first report on the isolation of a type 2/type 3 poliovirus capsid recombinant with one of the five crossover sites located in the *VP1* coding region.

Received 8 June 2009
Accepted 15 October 2009

INTRODUCTION

Polioviruses have three serotypes and are members of the human enterovirus C species that belong to the genus *Enterovirus* in the family *Picornaviridae* (Stanway *et al.*, 2005). Polioviruses have a positive-sense, single-stranded polyadenylated RNA genome, which is one of the smallest genomes among viruses (7500 nt), enclosed in an icosohedral capsid comprising 60 copies of each capsid protein (VP4, VP2, VP3 and VP1). The viral RNA contains a long ORF flanked by a 5′-untranslated region (UTR) and a 3′-UTR. A single polyprotein translated from the RNA strand is first cleaved into three polyprotein precursors: P1, P2 and P3. P1 is processed to yield four capsid proteins: VP4 to VP1. P2 and P3 are the precursors of non-structural proteins 2A–2C and 3A–3D (Wimmer *et al.*, 1993).

†These authors contributed equally to this work.

The GenBank/EMBL/DDBJ accession number for the complete genomic sequence of the natural intertypic type 2/type 3 capsid penta-recombinant VDPV sequence is AY948201.

A supplementary table of primer sequences is available with the online version of this paper.

Polioviruses are among the most important and well-studied human pathogens, since they are the causative agents of acute paralytic poliomyelitis. To control the incidence of infection, the trivalent oral polio vaccine (OPV) containing three live attenuated strains of the poliovirus serotypes (Sabin 1, Sabin 2 and Sabin 3) has been widely used in the global polio eradication program. Although OPV is safe, problems have occurred due to its ability to revert from the attenuated phenotype. Consequently, the vaccine is associated with a low rate of paralytic poliomyelitis (vaccine-associated paralytic poliomyelitis; VAPP) (Dowdle *et al.*, 2003). Further, polioviruses can also circulate invisibly without symptomatic patients in the population for several months and then revert from the attenuating form to a neurovirulent one (vaccine-derived polioviruses; VDPVs), causing outbreaks (Kew *et al.*, 2002; Liang *et al.*, 2006; Rousset *et al.*, 2003; Shimizu *et al.*, 2004; Yang *et al.*, 2003).

In the WHO program for the global eradication of poliomyelitis (WHO, 2004a), VDPVs have been classified into three categories. (i) Circulating VDPVs (cVDPVs). These are associated with sustained person–person transmission. They represent the strains showing $\leqslant$99 % *VP1* sequence homology to the ancestral Sabin OPV strains, and have caused paralytic cases in which related but non-identical viruses have been isolated (Kew *et al.*, 2004). (ii) Immunodeficiency VDPVs (iVDPVs). These represent strains with $\leqslant$99 % *VP1* sequence homology to the ancestral Sabin OPV strains, and are known to be excreted for a prolonged period from the same immunodeficient patient (Bellmunt *et al.*, 1999; Kew *et al.*, 1998). (iii) Ambiguous VDPVs (aVDPVs). These include other VDPVs that cannot be classified into the above two VDPV categories. These are viruses that either have been isolated from a single patient without immunodeficiency or are environmental isolates with an unidentified source (Kew *et al.*, 2005). Two genetic characteristics, nucleotide mutations and genetic rearrangements, seem to underlie the occurrence of poliomyelitis outbreaks associated with cVDPVs (Kew *et al.*, 2002, 2004, 2005).

While the genetic variability of polioviruses is mostly due to nucleotide substitutions resulting from a high error frequency during the replication of the viral RNA (Freistadt *et al.*, 2007), genetic changes in polioviruses can also occur during the molecular genomic rearrangements that happen during virus replication (Cuervo *et al.*, 2001). Poliovirus genomic rearrangement frequently takes place through homologous RNA recombination, mainly in the non-structural coding regions of the viral genome. Trivalent OPV permits co-infection of human gut cells with the Sabin 1, Sabin 2 and Sabin 3 strains, creating ideal conditions for intertypic recombination events. Analysis of VAPP infection cases revealed poliovirus recombination with a 50 % involvement of Sabin 2 strains and 67 % of Sabin 3 strains, while Sabin 1 strains were rarely involved (Furione *et al.*, 1993). Most crossover sites of the type 2 recombinants (S2/S1 and S2/S3 recombinants) lie in the *P3* coding region, and most crossover sites of type 3 recombinants (S3/S1 and S3/S2 recombinants) are located in the *P2* coding region (Cuervo *et al.*, 2001; Karakasiliotis *et al.*, 2004).

In this study, we describe a natural intertypic type 2/type 3 penta-recombinant VDPV isolated in 1997 from a patient with acute flaccid paralysis (AFP) during virological surveillance in China. Primary characterization of the isolate revealed that this VDPV has uncommon genetic rearrangements which include a crossover site in the *VP1* capsid genomic region. This observation led us to study the primary structure of the crossover sites and the genetic and phenotypic properties of this unusual poliovirus recombinant.

RESULTS

Primary characterization of strain CHN1025

Strain CHN1025 was completely neutralized with polyclonal antisera specific for type 2 but could not be neutralized with antisera for types 1 and 3. Thus, it was identified as a type 2 poliovirus. Intratypic differentiation (ITD) tests were performed by using two different methods. The PCR-RFLP ITD test revealed atypical Sabin 2 restriction patterns, and in the ELISA ITD test, the isolate was identified as SL, which indicated that it reacted with only Sabin 2-specific cross-absorbed rabbit antisera.

The entire *VP1* coding sequences of strain CHN1025 revealed an uncommon genomic intertypic (type 2/type 3) recombinant structure, with a crossover site within the *VP1* capsid coding region. The last 31 nt at the 3′ end of the *VP1* coding region were found to have high similarity (2 nt substitutions) with the Sabin 3 strain, while the rest of the *VP1* coding region had high similarity with the Sabin 2 strain (8 nt substitutions). These similarities indicated its VDPV genomic features (a total of 10 nt substitutions in 903 nt in the entire *VP1* coding region; homology with the relative Sabin strains was 98.9 %) and revealed that a crossover site was located in the *VP1* coding region (Table 1).

Penta-recombinant structure of the CHN1025 genome

Comparing the complete genomic sequence of strain CHN1025 (7440 nt) with that of the reference Sabin 2 strain (GenBank accession no. AY184220) revealed that at least five successive rounds of recombination events occurred in the genome in the *VP1* capsid coding region and *2C*, *3C* (twice) and $3D^{pol}$ non-capsid coding regions during its evolution.

Strain CHN1025 was a type 2/type 3 penta-recombinant VDPV with uncommon genetic rearrangements which include a crossover in the capsid genomic region. Based on its genomic organization, it is characterized as a S2/S3/S1/S3/S1/S3 penta-recombinant, and the complete genomic

Table 1. Nucleotide and amino acid substitutions in the penta-recombinant virus strain CHN1025 (GenBank accession no. AY948201) compared with Sabin 2, Sabin 3 and Sabin 1

Nucleotide and amino acid positions are numbered according to Sabin 2 (AY184220). Nucleotide or amino acid positions described as being involved in Sabin 2 attenuation are in bold. There are 10 nucleotide substitutions in the entire *VP1* coding region; the first eight are located before the crossover site within the *VP1* coding region and the other two are located after the crossover site.

Origin or donor	Region	Nucleotide			Amino acid			Phenotype
		Position	Sabin	CHN1025	Position	Sabin	CHN1025	
Sabin 2	5′-UTR	49	U	C				
		96*	–*	U				
		156	U	C				
		169	U	C				
		398	U	C				
		402	A	U				
		481	**A**	**G**				Attenuation
		663	U	C				
		707	A	G				
		730	U	C				
	VP4	809	G	A				
		810	C	U	21	Asp	Gly	
		863	A	G	39	Ser	Asn	
	VP2	1014	U	C				
		1038	G	A				
		1530	U	C				
	VP3	2118	C	A				
	VP1	2520	U	C				
		2538	U	C				
		2583	U	C				
		2682	C	U				
		2877	G	A	132	Ile	Met	
		2909	**U**	**C**	**143**	**Thr**	**Ile**	Attenuation
		3042	U	C				
		3304	C	A				
Sabin 3		3361	U	C				
		3378	C	U				
	2A	3708	C	U				
	2C	4473	A	C	117	Asn	Lys	
		4500	A	G				
		4551	U	C				
Sabin 1				No substitutions				
Sabin 3				No substitutions				
Sabin 1	3C	5799	A	G				
Sabin 3	3D	6429	C	U				
		6513	U	A				
		6969	C	U				
		7002	C	U				
		7353	U	A				

*There is a U insertion at nt 96 in the 5′-UTR of strain CHN1025 compared with Sabin strain. There is no relevant base in Sabin strain.

sequence revealed the presence of five crossover sites. The first apparently occurred from an S2/S3 recombination event, with the crossover site located between nt 3354 and nt 3356 in the *VP1* coding region, while the second crossover site was from an S3/S1 recombination event located between nt 4888 and nt 4895 in the *2C* coding region. The third and fourth crossover sites were from S1/S3 and S3/S1 recombination events, with the two crossover sites located in nt 5447–5493 and nt 5671–5690 in the *3C* coding region, respectively. The last crossover site was from another S1/S3 recombination event located between nt 6064 and nt 6092 in the $3D^{pol}$ coding region (Fig. 1).

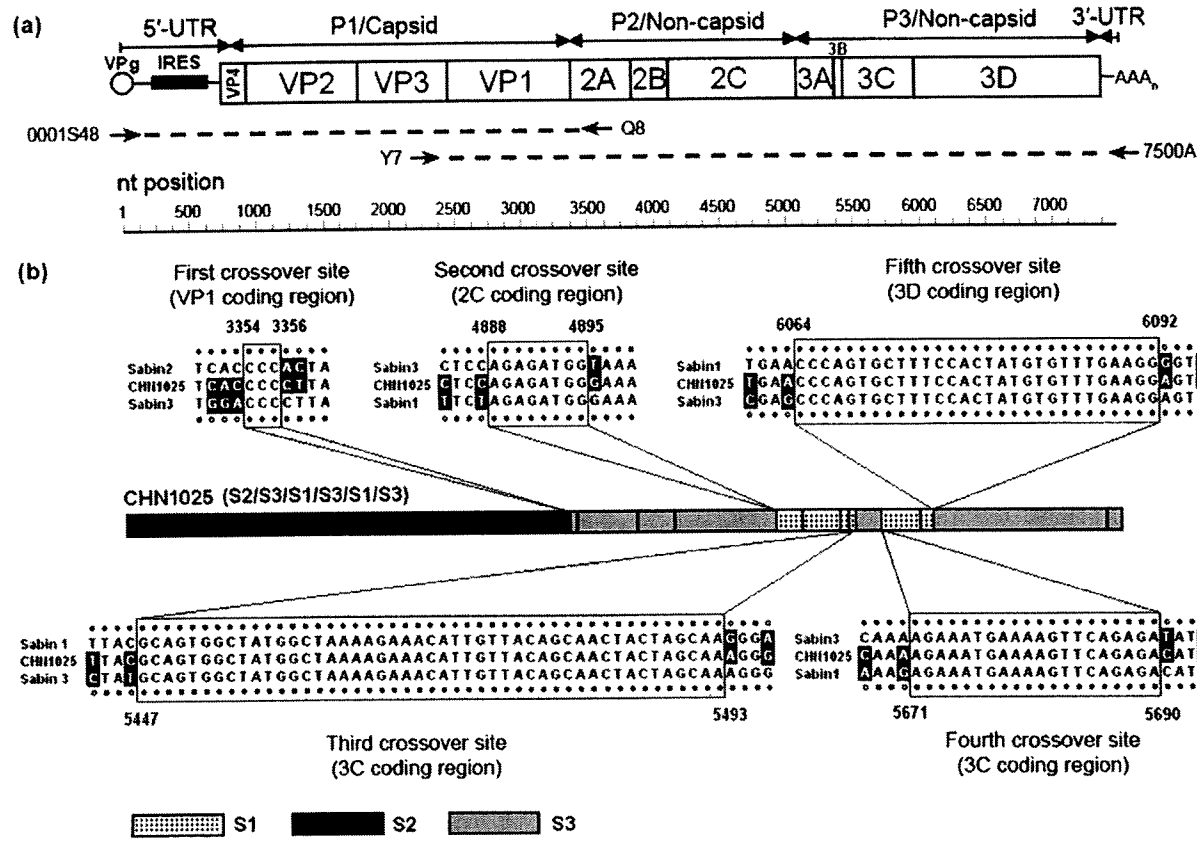

Fig. 1. Schematic genomic structure of CHN1025. (a) The primer pairs for two long distance PCR amplifications to obtain the whole genome sequence of CHN1025. (b) The five proposed crossover sites are shown in detail. The last nucleotides, differentiating the sequence of CHN1025 from the 3′ partner reference sequences, and the first nucleotides, differentiating the sequence of CHN1025 from the 5′ partner reference sequence, i.e. the crossover sites, are highlighted by black shading. The filled circles and open circles above and below the nucleotide sequences, respectively, indicate the same and different bases between the sequence of CHN1025 and the partner reference sequences.

Replacement of attenuating determinants by back mutation

The complete genomic sequence of strain CHN1025 showed that its genome was collinear with that of the Sabin 2 strain, except for an insertion U at nt 96 in the 5′-UTR, suggesting that recombination did not alter the total number of capsid codons. A total of 37 nt substitutions were distributed throughout the genome, but most of them were located in the 5′-UTR (10 mutations out of total 748 nt; 1.34%) and P1/capsid-coding region (17 mutations out of total 2637 nt; 0.64%) (Table 1). The five crossover sites divided the genome into six parts, and most of the nucleotide substitutions (25 mutations out of total 3357nt; 0.74%) were located in the first part of the original sequence; a small portion (12 mutations out of 4083 nt; 0.29%) were present in the five parts of the donor sequences. The donor sequences of Sabin 1 between the second and the third crossover sites, and Sabin 3 sequence between the third and the fourth crossover sites contained no nucleotide substitutions compared with the relevant sequences of the relative Sabin strain (Table 1).

The nucleotide substitutions that had been identified as the principal determinants of the attenuated phenotype of the Sabin 2 strain had reverted through a transition A-to-G reversion at nt 481 in the 5′-UTR and a transition U-to-C reversion at nt 2909 in the *VP1* coding region, leading to a Thr-to-Ile amino acid substitution of residue 143 in VP1 in isolate CHN1025 (Minor *et al.*, 1993; Ren *et al.*, 1991) (Table 2). Both replacements restored the consensus residues for the prototype wild-type 2 poliovirus strain MEF-1/EGY/1942.

Antigenic properties of the penta-recombinant VDPV

Antigenic analyses performed by the ELISA ITD method with cross-absorbed antisera characterized the type 2

Table 2. Neurovirulence of isolate CHN1025 in PVR-Tg21 transgenic mice

ND, Not done.

Isolate	No. of mice killed out of total no. inoculated with a dose ($TCID_{50}$ per mouse) of:					PD_{50}*
	5.5	4.5	3.5	2.5	1.5	
CHN1025	ND	1/6	1/6	0/6	0/6	⩾4.7
MEF-1	ND	ND	6/6	5/6	0/3	2.2

*Values represent the virus titre that induced paralysis or death in 50 % of inoculated mice (PD_{50}) and are expressed as a multiple of the $TCID_{50}$.

isolate CHN1025 as a Sabin-like virus. The amino acid sequences within or near the predicted neutralizing antigenic (NAg) sites (Minor, 1990) were aligned with the penta-recombinant VDPV, Sabin 2 strain, two Egypt type 2 cVDPV strains (GenBank accession nos AF448782 and AF448783) (Yang *et al.*, 2003), two Madagascar type 2 cVDPV strains (GenBank accession nos AM084223 and AM084225) (Rakoto-Andrianarivelo *et al.*, 2007), two Spain type 2 iVDPV strains (GenBank accession nos EU566941 and EU566950) (Avellón *et al.*, 2008) and the prototype wild-type 2 poliovirus strain MEF-1/EGY/1942. There were no amino acid substitutions in the NAg sites among the penta-recombinant VDPV, which coincided with the results of ELISA ITD (Fig. 2), and no amino acid changes were introduced in the *VP1* capsid coding region as a consequence of the observed recombination (Table 1). Sabin-specific epitopes were present in strain CHN1025, suggesting that the virus was antigenically indistinguishable from the Sabin 2 reference strain. Although none of the amino acid substitutions are located in the NAg sites described so far, some are exposed on the virion surface, including residue 143 of VP1 which is in loop D–E (Lentz *et al.*, 1997).

Neurovirulence of isolate CHN1025 in PVR-Tg21 transgenic mice

Isolate CHN1025 was isolated from a patient with AFP, demonstrating their neurovirulence for humans under natural conditions. The neurovirulence of isolate CHN1025 was examined in PVR-Tg21 transgenic mice expressing the human receptor for poliovirus and compared with the neurovirulence of Sabin 2 and the prototype wild-type 2 MEF-1/EGY/1942 strain. Under the assay conditions, MEF-1/EGY/1942 showed maximum neurovirulence, and the virus titre that induced paralysis or death in 50 % of the inoculated mice (PD_{50}) was 2.2, while isolate CHN1025 partially regained the neurovirulence characteristics of MEF-1/EGY/1942, as determined by PD_{50} measurements, with a PD_{50} value of ⩾4.7 (Table 2).

Estimated evolution time of the capsid penta-recombinant

The approximate duration of replication of the capsid penta-recombinant VDPV after the initiating vaccine dose was estimated from the P1/capsid sequence difference

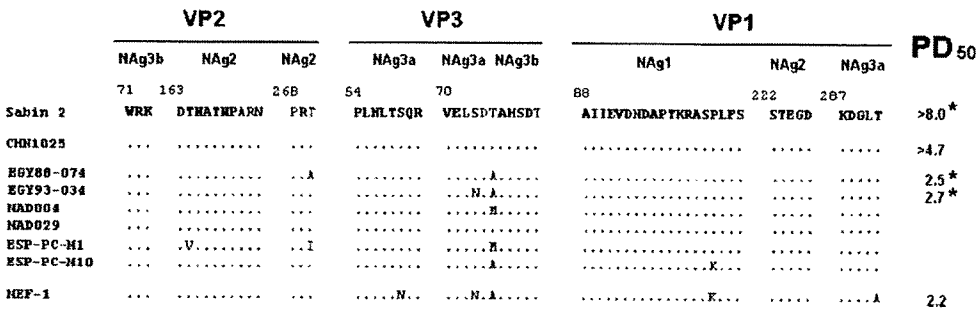

Fig. 2. Alignment of amino acid residues of NAg sites 1 (*VP1*, 88–106), 2 (*VP2*, 163–172; *VP2*, 268–270; *VP1*, 222–227), 3a (*VP3*, 54–61; *VP3*, 70–74; *VP1*, 287–292) and 3b (*VP2*, 71–73; *VP3*, 75–80) for Sabin 2, CHN1025, Egypt type 2 cVDPV strains (GenBank accession nos AF448782 and AF448783), Madagascar type 2 cVDPV strains (GenBank accession nos AM084223 and AM084225), Spain type 2 iVDPV strains (GenBank accession nos EU566941 and EU566950) and the prototype wild-type 2 poliovirus strain, MEF-1/EGY/1942. The PD_{50} values of Egypt type 2 cVDPV strains are taken from a report by Yang *et al.* (2003).

between isolate CHN1025 and the Sabin 2 strain. The corrected proportion of synonymous substitutions (K_s) was 1.35% of synonymous sites in the P1/capsid region (not including the donor recombinant sequences) and that of total substitutions (K_t) was 0.58%. Under the assumption of constant nucleotide substitution rates of 3.2% synonymous substitutions per synonymous sites per year and 1.1% total substitutions per site per year in the P1/capsid region (Jorba *et al.*, 2008), we estimated that the age of the capsid penta-recombinant VDPV was 154 days (from the K_s estimate) and 192 days (from the K_t estimate), respectively (Fig. 3). By comparing the calculated range of the estimation of initiating OPV dose with the epidemiological data, we estimated that the five successive rounds of recombination events most likely occurred between late July 1996 and early February 1997 (Fig. 3).

DISCUSSION

In this paper, we describe an intertypic type 2/type 3 penta-recombinant poliovirus (strain CHN1025) isolated from a patient with AFP in the Shandong Province of China; the first crossover site in this virus was located in the *VP1* coding region. Because this patient did not receive any dose of OPV after birth, the illness was caused by a poliovirus variant infection. Strain CHN1025 was identified as a type 2/type 3 penta-recombinant poliovirus with five crossover sites in its genome, which include a crossover site in the *VP1* capsid genomic region, and most of the characteristics of the type 2 vaccine strain, such as antigenic properties in

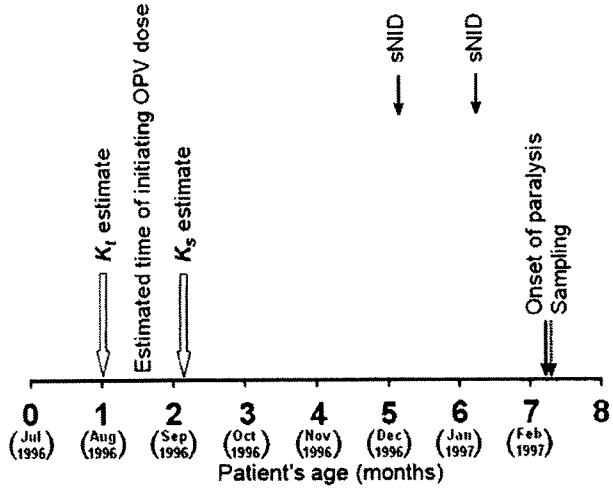

Fig. 3. Time line showing the date of birth of the patient with AFP, the dates of the subsequent sub-national immunization day (sNID; the day of an intensive immunization campaign when all children under 5 years old are targeted to receive vaccination against polio) in Shandong Province, the date of onset of AFP, the date of sampling and the estimated dates of the OPV dose that initiated VDPV replication.

ELISA ITD with cross-absorbed antisera (van der Avoort *et al.*, 1995), the same NAg sites and moderate neurovirulence. Despite these similarities, nucleotide sequencing showed a 1.1% nucleotide variation in the *VP1* coding region, so strain CHN1025 was identified as a VDPV. According to the WHO program of global eradication of poliomyelitis (WHO, 2004a), this VDPV is undoubtedly an aVDPV, because it does not have the genetic characteristics of iVDPV, such as numerous amino acid changes in NAg sites (Bellmunt *et al.*, 1999; Kew *et al.*, 1998).

To the best of our knowledge, this is the first report of a type 2/type 3 penta-recombinant VDPV which includes a crossover site in the *VP1* capsid coding region. Recombination among OPV strains is easily detectable because the sequences of the parental vaccine strains are well defined (Toyoda *et al.*, 1984). Natural recombination in polioviruses was first recognized when viruses with chimeric non-capsid sequences were isolated from children exposed to the OPV (Cammack *et al.*, 1988). Although studies of polioviruses isolated from patients with poliomyelitis have demonstrated a high frequency of genetic recombination (Guillot *et al.*, 2000), the recombinant polioviruses described here are unusual because they have five crossover sites including a crossover site within the *VP1* capsid coding region of their genome, while crossover sites in the intertypic recombinants excreted by children exposed to OPV are usually restricted to the *P2* or *P3* non-capsid region (Cammack *et al.*, 1988; Cuervo *et al.*, 2001). No natural type 2/type 3 intertypic recombinants with a crossover site in *VP1* coding region have been reported previously, and only few natural intertypic capsid-recombinant polioviruses have been reported. All reports have been on type 3/type 2 intertypic recombinants (Blomqvist *et al.*, 2003; Dedepsidis *et al.*, 2008; Martín *et al.*, 2002). Natural intertypic recombination with a crossover site in the capsid coding region is a rare phenomenon, and no amino acid changes are introduced in the *VP1* capsid region as a consequence of the observed recombination, possibly due to structural constraints that exist to maintain the integrity of the capsid shell. The integrity of the capsid region of poliovirus seems to be very important for propagation of the viruses themselves (Kohara *et al.*, 1988).

A small portion of the nucleotide substitutions located in the donor sequences, two in particular, contained no nucleotide substitutions, suggesting that the donor sequences were relatively new. At least five successive rounds of recombination events occurred in the CHN1025 genome over a relatively short time period. This view was reinforced by the estimates of the apparent viral infection, which indicated that this occurred within 154 days (from the K_s estimate) and 192 days (from the K_t estimate) before the sampling dates. This is about the time of two rounds of mass immunization campaigns in Shandong Province, so there is a possibility that the virus was acquired by the patient from contact with a vaccine recipient, but unfortunately there is no way to test this possibility in this case, since additional stool specimens were not

available from the patient's close contacts. The VDPV may infect the patient later in life, possibly close to the time of paralysis, and the exact source of the VDPV was unknown, as routine OPV coverage was high in Shandong Province in 1997 (Fig. 3).

The result of a neurovirulence test for isolate CHN1025 performed on PVR-Tg21 transgenic mice showed that MEF-1 virus is significantly more neurovirulent than strain CHN1025. Even though nucleotide substitutions at positions 481 of the 5′-UTR and 2909 of *VP1* coding region (aa 143), regions known to be neurovirulence determinants, were present in the genome, moderate neurovirulence was observed in the transgenic mice. This observation may have been because the neurovirulence determinants of type 2 polioviruses do not strictly correlate with those in transgenic mice (Buttinelli *et al.*, 2003).

Because the base substitutions contributing to the attenuated phenotype of the Sabin 2 strain readily revert during replication in the human gut, the viruses excreted by healthy vaccinees are frequently less attenuated than the original OPV strains (Macadam *et al.*, 1993). Reversion is very rapid for the Sabin 2 strain because attenuation is primarily determined by only two highly unstable substitutions (Minor *et al.*, 1993; Ren *et al.*, 1991). The intense selection against the attenuating mutations suggested that the revertants replicate more efficiently in the human gut (Minor & Dunn, 1988). Therefore, it appears likely that isolate CHN1025, a Sabin 2 revertant, with increased potential for neurovirulence and transmissibility, is selected in communities where OPV is used, such as in Shandong Province. However, their spread in Shandong Province was restricted by the high population immunity (Yang *et al.*, 2003).

It is known that the type 2 OPV strain spreads to unvaccinated children more easily than the other two serotypes (Fine & Carneiro, 1999). Therefore, this biological feature would favour its divergence and emergence as a paralysis-causing pathogen to unvaccinated children. Determining whether neurovirulence and transmissibility of VDPVs could be the result of the recombination remains to be elucidated. Indeed, VDPVs will become increasingly important as the prevalence of wild polioviruses decreases and OPV becomes the only remaining source of poliovirus infection, and as VDPVs can emerge in any country that uses OPV with insufficient vaccine coverage. The recent VDPV outbreaks also highlight the importance of maintaining sensitive poliovirus laboratory surveillance. Such surveillance will have major implications for the cessation of immunization with OPV after it is certified that wild polioviruses have been eradicated.

METHODS

Patient history and clinical specimens. A type 2 poliovirus recombinant (strain CHN1025) was isolated from a 7-month-old boy from Chiping County (population: ~570 000) of Shandong Province, China, who developed clinical symptoms of muscular weakness, hypotony and paralysis on 3 February 1997. The patient was not known to have ever received a dose of OPV after birth and showed no signs of immunodeficiency at the time of presentation (data not shown). Two stool specimens were collected from the patient at a 24 h interval on 6–7 February 1997. He had residual paralysis at the 60 day clinical follow-up and his condition was classified as AFP by the Shandong provincial and National polio diagnosis experts group.

Viral isolation and primary identification. Human rhabdomyosarcoma and L20B (a mouse cell line carrying the human poliovirus receptor) cell lines were used to isolate viruses from the stool specimens by standard methods (WHO, 2004b). Isolates were initially characterized by a micro-neutralization assay using poliovirus type-specific rabbit polyclonal antisera [National Institute for Public Health and the Environment (RIVM), Bilthoven, The Netherlands] (WHO, 2004b). ITD was performed using the PCR-RFLP (Balanant *et al.*, 1991) and ELISA (van der Avoort *et al.*, 1995) methods in order to investigate the wild or vaccine origin of the poliovirus isolate.

Viral RNA extraction and reverse transcription. Viral RNA was extracted from the viral isolate using a QIAamp viral RNA mini kit (Qiagen) and stored at −80 °C until further use. SuperScript II RNase H^- reverse transcriptase [1 μl (200 U); Invitrogen] was used to produce single-stranded cDNA from 5 μl purified viral RNA. The cDNA synthesis was primed by using primers 7500A and Q8 (Fig. 1a; Supplementary Table S1, available in JGV Online), respectively, and performed at 42 °C for 2 h, followed by 60 °C for 15 min to inactivate the enzyme. Finally, RNA in an RNA : DNA hybrid was specifically degraded with 1 μl RNase H (Promega) at 37 °C for 30 min.

Full-length genome amplification. Two long-distance PCR amplifications were performed by using the *Taq*Plus Precision PCR system (Stratagene), which consists of a blend of Stratagene cloned *Pfu* DNA polymerase (proof-reading) and *Taq*2000 DNA polymerase (non-proof-reading). Reactions contained 5 μl cDNA (see above), 0.1 mM each dNTP, 10 μl *Taq*Plus buffer, 1.0 ng μl^{-1} forward (0001S48 or Y7) and reverse (Q8 or 7500A) primers (Fig. 1a; Supplementary Table S1) and 5 U *Taq*Plus enzyme in a 100 μl reaction. The amplification was carried as follows: 30 cycles of 94 °C (30 s), 60 °C (30 s) and 72 °C (6 min), followed by 94 °C (1 min) and 72 °C (20 min).

Nucleotide sequencing. Two long-distance PCR products were purified using a QIAquick gel extraction kit (Qiagen). Cycle sequencing reactions were carried out using the version 3.0 of the BigDye terminator chemistry (Applied Biosystems), using the primers listed in Supplementary Table S1. Sequencing was performed in both directions using an ABI PRISM 3100 Genetic Analyzer (Applied Biosystems), and every nucleotide position was sequenced at least once from each strand. The 5′ segment sequences were determined by using the 5′ rapid amplification of cDNA ends (RACE) core set (TaKaRa Biomedicals) according to the manufacturer's instructions.

Location of the crossover sites. The sequences of the isolates were aligned with the reference strains by using MEGA program v4.0 (Sudhir Kumar, Arizona State University, Arizona, USA) (Tamura *et al.*, 2007); the resulting reference strain sequences were found to be sequences with the GenBank accession nos AY184219, AY184220 and AY184221 for Sabin 1, Sabin 2 and Sabin 3, respectively. Plots of nucleotide similarity were created using SimPlot program v3.5.1 (Stuart Ray, Johns Hopkins University, Baltimore, Maryland, USA) (Lole *et al.*, 1999). The crossover sites were identified as being located between the last nucleotide, differentiating the clinical sequence from the 3′ partner reference sequences, and the first nucleotide,

differentiating the clinical sequence from the 5′ partner reference sequence.

Neurovirulence testing in PVR-Tg21 transgenic mice. A neurovirulence test was carried out using PVR-Tg21 mice that expressed the human poliovirus receptor (CD155) (Georgescu *et al.*, 1997). The type 2 reference Sabin attenuated strain [obtained from the National Institute for Biological Standard and Control (NIBSC), UK] and prototype wild-type 2 neurovirulent MEF-1 strain [obtained from the National Institute of Infectious Diseases (NIID), Japan] were used as virus controls in the test. In brief, six mice (4-weeks-old; three males and three females) were inoculated intracerebrally with 30 µl each virus dilution [in 10-fold increments; ranging from 2.5 to 6.5 log 50 % cell culture infective dose ($CCID_{50}$) per mouse]. The mice were examined daily for 14 days after inoculation, and the number of paralysed or dead mice was recorded. The virus titre that induced paralysis or death in 50 % of the inoculated mice (PD_{50}) was calculated by using the Kärber formula (Kärber, 1931) and expressed as PD_{50} per mouse.

Estimating the date of the initiating OPV dose. The date of the initiating OPV dose for the AFP case patient described in this study was estimated from the K_s (synonymous substitutions per synonymous site) and K_t (total substitutions per site) values by assuming evolution rates of 0.032 synonymous substitutions per synonymous site per year and 0.011 total substitutions per site per year (Jorba *et al.*, 2008).

Nucleotide sequence accession number. The complete genomic sequence of the natural intertypic type 2/type 3 capsid penta-recombinant VDPV described in this study was deposited in the GenBank database under the accession number AY948201.

ACKNOWLEDGEMENTS

We thank Dr. Chen-Fu Yang and Dr. Kew Olen for kindly sharing some nucleotide sequences for primers. This study was supported by the National Key Technology R&D Program of China (Project no. 2008BAI56B00), National Key Science and Technology Projects of China (Project no. 2008ZX10004-008) and grant I8/181/978 from the World Health Organization.

REFERENCES

Avellón, A., Cabrerizo, M., de Miguel, T., Pérez-Breña, P., Tenorio, A., Pérez, J. L., de Aragón, M. V. & Trallero, G. (2008). Paralysis case and contact spread of recombinant vaccine-derived poliovirus, Spain. *Emerg Infect Dis* **14**, 1807–1809.

Balanant, J., Guillot, S., Candrea, A., Delpeyroux, F. & Crainic, R. (1991). The natural genomic variability of poliovirus analyzed by a restriction fragment length polymorphism assay. *Virology* **184**, 645–654.

Bellmunt, A., May, G., Zell, R., Pring-Akerblom, P., Verhagen, W. & Heim, A. (1999). Evolution of poliovirus type 1 during 5.5 years of prolonged enteral replication in an immunodeficient patient. *Virology* **265**, 178–184.

Blomqvist, S., Bruu, A. L., Stenvik, M. & Hovi, T. (2003). Characterization of a recombinant type 3/type 2 poliovirus isolated from a healthy vaccinee and containing a chimeric capsid protein VP1. *J Gen Virol* **84**, 573–580.

Buttinelli, G., Donati, V., Fiore, S., Marturano, J., Plebani, A., Balestri, P., Soresina, A. R., Vivarelli, R., Delpeyroux, F. & other authors (2003). Nucleotide variation in Sabin type 2 poliovirus from an immunodeficient patient with poliomyelitis. *J Gen Virol* **84**, 1215–1221.

Cammack, N., Phillips, A., Dunn, G., Patel, V. & Minor, P. D. (1988). Intertypic genomic rearrangements of poliovirus strains in vaccinees. *Virology* **167**, 507–514.

Cuervo, N. S., Guillot, S., Romanenkova, N., Combiescu, M., Aubert-Combiescu, A., Seghier, M., Caro, V., Crainic, R. & Delpeyroux, F. (2001). Genomic features of intertypic recombinant Sabin poliovirus strains excreted by primary vaccinees. *J Virol* **75**, 5740–5751.

Dedepsidis, E., Pliaka, V., Kyriakopoulou, Z., Brakoulias, C., Levidiotou-Stefanou, S., Pratti, A., Mamuris, Z. & Markoulatos, P. (2008). Complete genomic characterization of an intertypic Sabin 3/Sabin 2 capsid recombinant. *FEMS Immunol Med Microbiol* **52**, 343–351.

Dowdle, W. R., De Gourville, E., Kew, O. M., Pallansch, M. A. & Wood, D. J. (2003). Polio eradication: the OPV paradox. *Rev Med Virol* **13**, 277–291.

Fine, P. E. & Carneiro, I. A. (1999). Transmissibility and persistence of oral polio vaccine viruses: implications for the global poliomyelitis eradication initiative. *Am J Epidemiol* **150**, 1001–1021.

Freistadt, M. S., Vaccaro, J. A. & Eberle, K. E. (2007). Biochemical characterization of the fidelity of poliovirus RNA-dependent RNA polymerase. *Virol J* **4**, 44.

Furione, M., Guillot, S., Otelea, D., Balanant, J., Candrea, A. & Crainic, R. (1993). Polioviruses with natural recombinant genomes isolated from vaccine-associated paralytic poliomyelitis. *Virology* **196**, 199–208.

Georgescu, M. M., Balanant, J., Macadam, A., Otelea, D., Combiescu, M., Combiescu, A. A., Crainic, R. & Delpeyroux, F. (1997). Evolution of the Sabin type 1 poliovirus in humans: characterization of strains isolated from patients with vaccine-associated paralytic poliomyelitis. *J Virol* **71**, 7758–7768.

Guillot, S., Caro, V., Cuervo, N., Korotkova, E., Combiescu, M., Persu, A., Aubert-Combiescu, A., Delpeyroux, F. & Crainic, R. (2000). Natural genetic exchanges between vaccine and wild poliovirus strains in humans. *J Virol* **74**, 8434–8443.

Jorba, J., Campagnoli, R., De, L. & Kew, O. (2008). Calibration of multiple poliovirus molecular clocks covering an extended evolutionary range. *J Virol* **82**, 4429–4440.

Karakasiliotis, I., Markoulatos, P. & Katsorchis, T. (2004). Site analysis of recombinant and mutant poliovirus isolates of Sabin origin from patients and from vaccinees. *Mol Cell Probes* **18**, 103–109.

Kärber, G. (1931). Beitrag zur kollektiven Behandlung pharmakologischer Reihenversuche. *Naunyn Schmiedebergs Arch Pharmacol* **162**, 480–483 (in German).

Kew, O. M., Sutter, R. W., Nottay, B. K., McDonough, M. J., Prevots, D. R., Quick, L. & Pallansch, M. A. (1998). Prolonged replication of a type 1 vaccine-derived poliovirus in an immunodeficient patient. *J Clin Microbiol* **36**, 2893–2899.

Kew, O., Morris-Glasgow, V., Landaverde, M., Burns, C., Shaw, J., Garib, Z., André, J., Blackman, E., Freeman, C. J. & other authors (2002). Outbreak of poliomyelitis in Hispaniola associated with circulating type 1 vaccine-derived poliovirus. *Science* **296**, 356–359.

Kew, O. M., Wright, P. F., Agol, V. I., Delpeyroux, F., Shimizu, H., Nathanson, N. & Pallansch, M. A. (2004). Circulating vaccine-derived polioviruses: current state of knowledge. *Bull World Health Organ* **82**, 16–23.

Kew, O. M., Sutter, R. W., de Gourville, E. M., Dowdle, W. R. & Pallansch, M. A. (2005). Vaccine-derived polioviruses and the endgame strategy for global polio eradication. *Annu Rev Microbiol* **59**, 587–635.

Kohara, M., Abe, S., Komatsu, T., Tago, K., Arita, M. & Nomoto, A. (1988). A recombinant virus between the Sabin 1 and Sabin 3 vaccine strains of poliovirus as a possible candidate for a new type 3 poliovirus live vaccine strain. *J Virol* **62**, 2828–2835.

Lentz, K. N., Smith, A. D., Geisler, S. C., Cox, S., Buontempo, P., Skelton, A., DeMartino, J., Rozhon, E., Schwartz, J. & other authors (1997). Structure of poliovirus type 2 Lansing complexed with antiviral agent SCH48973: comparison of the structural and biological properties of three poliovirus serotypes. *Structure* 5, 961–978.

Liang, X., Zhang, Y., Xu, W., Wen, N., Zuo, S., Lee, L. A. & Yu, J. (2006). An outbreak of poliomyelitis caused by type 1 vaccine-derived poliovirus in China. *J Infect Dis* **194**, 545–551.

Lole, K. S., Bollinger, R. C., Paranjape, R. S., Gadkari, D., Kulkarni, S. S., Novak, N. G., Ingersoll, R., Sheppard, H. W. & Ray, S. C. (1999). Full-length human immunodeficiency virus type 1 genomes from subtype C-infected seroconverters in India, with evidence of intersubtype recombination. *J Virol* **73**, 152–160.

Macadam, A. J., Pollard, S. R., Ferguson, G., Skuce, R., Wood, D., Almond, J. W. & Minor, P. D. (1993). Genetic basis of attenuation of the Sabin type 2 vaccine strain of poliovirus in primates. *Virology* **192**, 18–26.

Martín, J., Samoilovich, E., Dunn, G., Lackenby, A., Feldman, E., Heath, A., Svirchevskaya, E., Cooper, G., Yermalovich, M. & Minor, P. D. (2002). Isolation of an intertypic poliovirus capsid recombinant from a child with vaccine-associated paralytic poliomyelitis. *J Virol* **76**, 10921–10928.

Minor, P. D. (1990). Antigenic structure of picornaviruses. *Curr Top Microbiol Immunol* **161**, 121–154.

Minor, P. D. & Dunn, G. (1988). The effect of sequences in the 5′ non-coding region on the replication of polioviruses in the human gut. *J Gen Virol* **69**, 1091–1096.

Minor, P. D., Macadam, A. J., Stone, D. M. & Almond, J. W. (1993). Genetic basis of attenuation of the Sabin oral poliovirus vaccines. *Biologicals* **21**, 357–363.

Rakoto-Andrianarivelo, M., Guillot, S., Iber, J., Balanant, J., Blondel, B., Riquet, F., Martín, J., Kew, O., Randriamanalina, B. & other authors (2007). Co-circulation and evolution of polioviruses and species C enteroviruses in a district of Madagascar. *PLoS Pathog* **3**, e191.

Ren, R. B., Moss, E. G. & Racaniello, V. R. (1991). Identification of two determinants that attenuate vaccine-related type 2 poliovirus. *J Virol* **65**, 1377–1382.

Rousset, D., Rakoto-Andrianarivelo, M., Razafindratsimandresy, R., Randriamanalina, B., Guillot, S., Balanant, J., Mauclere, P. & Delpeyroux, F. (2003). Recombinant vaccine-derived poliovirus in Madagascar. *Emerg Infect Dis* **9**, 885–887.

Shimizu, H., Thorley, B., Paladin, F. J., Brussen, K. A., Stambos, V., Yuen, L., Utama, A., Tano, Y., Arita, M. & other authors (2004). Circulation of type 1 vaccine-derived poliovirus in the Philippines in 2001. *J Virol* **78**, 13512–13521.

Stanway, G., Brown, F., Christian, P., Hovi, T., Hyypiä, T., King, A. M. Q., Knowles, N. J., Lemon, S. M., Minor, P. D. & other authors (2005). Family *Picornaviridae*. In *Virus Taxonomy. Eighth Report of the International Committee on Taxonomy of Viruses*, pp. 757–778. Edited by C. M. Fauquet, M. A. Mayo, J. Maniloff, U. Desselberger & L. A. Ball. London: Elsevier.

Tamura, K., Dudley, J., Nei, M. & Kumar, S. (2007). MEGA4: Molecular Evolutionary Genetics Analysis (MEGA) software version 4.0. *Mol Biol Evol* **24**, 1596–1599.

Toyoda, H., Kohara, M., Kataoka, Y., Suganuma, T., Omata, T., Imura, N. & Nomoto, A. (1984). Complete nucleotide sequences of all three poliovirus serotype genomes. Implication for genetic relationship, gene function and antigenic determinants. *J Mol Biol* **174**, 561–585.

van der Avoort, H. G., Hull, B. P., Hovi, T., Pallansch, M. A., Kew, O. M., Crainic, R., Wood, D. J., Mulders, M. N. & van Loon, A. M. (1995). Comparative study of five methods for intratypic differentiation of polioviruses. *J Clin Microbiol* **33**, 2562–2566.

WHO (2004a). Global Polio Eradication Initiative, strategic plan 2004–2008. *Wkly Epidemiol Rec* **79**, 55–57.

WHO (2004b). *Polio Laboratory Manual*, 4th edn. Document WHO/IVB/04.10. Geneva, Switzerland: World Health Organization. www.who.int/vaccines/en/poliolab/WHO-Polio-Manual-9.pdf

Wimmer, E., Hellen, C. U. & Cao, X. (1993). Genetics of poliovirus. *Annu Rev Genet* **27**, 353–436.

Yang, C. F., Naguib, T., Yang, S. J., Nasr, E., Jorba, J., Ahmed, N., Campagnoli, R., van der Avoort, H., Shimizu, H. & other authors (2003). Circulation of endemic type 2 vaccine-derived poliovirus in Egypt from 1983 to 1993. *J Virol* **77**, 8366–8377.

Journal of Medical Virology 82:649–657 (2010)

A Comparison of the VP1, VP2, and VP4 Regions for Molecular Typing of Human Enteroviruses

David Perera,[1]* Hiroyuki Shimizu,[2] Hiromu Yoshida,[2] Phan Van Tu,[3] Hiroaki Ishiko,[4] Peter C. McMinn,[5] and Mary J. Cardosa[1]

[1]*Institute of Health & Community Medicine, Universiti Malaysia Sarawak, Kota Samarahan, Sarawak, Malaysia*
[2]*Department of Virology II, National Institute of Infectious Diseases, Tokyo, Japan*
[3]*Pasteur Institute of Ho Chi Minh City, Ho Chi Minh City, Vietnam*
[4]*Host Defense Laboratory, Mitsubishi Chemical Medicine Corporation, Tokyo, Japan*
[5]*Discipline of Infectious Diseases and Immunology, Central Clinical School, University of Sydney, Sydney, NSW, Australia*

The VP4, VP2, and VP1 gene regions were evaluated for their usefulness in typing human enteroviruses. Three published RT-PCR primers sets targeting separately these three gene regions were used. Initially, from a total of 86 field isolates (36 HEV-A, 40 HEV-B, and 10 HEV-C) tested, 100% concordance in HEV-A was identified from all three gene regions (VP4, VP2, and VP1). However, for HEV-B and HEV-C viruses, only the VP2 and VP1 regions, and not VP4, showed 100% concordance in typing these viruses. To evaluate further the usefulness of VP4 in typing HEV-A enteroviruses, 55 Japanese and 203 published paired VP4 and VP1 nucleotide sequences were also examined. In each case, typing by VP4 was 100% in concordance with typing using VP1. Given these results, it is proposed that for HEV-A enteroviruses, all three gene regions (VP4, VP2, and VP1), would be useful for typing these viruses. These options would enhance the capability of laboratories in identifying these viruses and would greatly help in outbreaks of hand, foot, and mouth disease. ***J. Med. Virol. 82:649–657, 2010.***

KEY WORDS: human enterovirus; RT-PCR detection; hand, foot, and mouth disease

INTRODUCTION

Human enteroviruses are small non-enveloped RNA viruses that belong to the family *Picornaviridae*. Classification of human enteroviruses using molecular methods has divided these viruses into dive separate species (poliovirus, HEV-A, HEV-B, HEV-C, and HEV-D) [Stanway et al., 2005]. To date 62 antigenically distinct serotypes and more than 30 additional genetically distinct types have been described (http://www.picornaviridae.com/enterovirus/enterovirus.htm). In the last decade, a succession of large outbreaks of hand, foot, and mouth disease (HFMD) has been reported in the Asia-Pacific region [McMinn, 2002; Cardosa et al., 2003; Miyazawa et al., 2008; Ang et al., 2009; Zhang et al., 2009]. Although, the disease is generally characterized as a mild childhood illness, recent outbreaks have shown that there can be severe symptoms that sometimes lead to fatal outcomes associated with human enterovirus 71 (HEV71), which belongs to the HEV-A species [McMinn, 2002]. HEV-A viruses are associated most commonly with HFMD outbreaks [Yamashita et al., 2005; Podin et al., 2006]. Of these, HEV71 and human coxsackievirus A16 (CVA16) are the viruses most often isolated from these outbreaks and co-circulation of both viruses during HFMD outbreaks is a frequent occurrence [Lin et al., 2003; Li et al., 2005; Podin et al., 2006; Hosoya et al., 2007]. Of the two, infection with CVA16 is associated with a milder form of the disease as compared with HEV71 which is associated with acute neurological symptoms in a small proportion of cases [Lin et al., 2003; Li et al., 2005; Podin et al., 2006]. In view of this, it is important to be able to identify the enterovirus serotype during HFMD outbreaks so that informed decisions on public health intervention and treatment can be made.

Several different RT-PCR methods targeting different regions of the enterovirus genome, particularly those encoding the structural proteins of the virus have been used to determine serotype identity [Casas et al., 2001;

Grant sponsor: The Wellcome Trust; Grant number: WT071588MA; Grant sponsor: Universiti Malaysia Sarawak (Operational Fund).

*Correspondence to: David Perera, Institute of Health & Community Medicine, Universiti Malaysia Sarawak, Kota Samarahan, 94300 Sarawak, Malaysia. E-mail: davidperera@yahoo.com

Accepted 11 August 2009
DOI 10.1002/jmv.21652
Published online in Wiley InterScience (www.interscience.wiley.com)

Ishiko et al., 2002; Oberste et al., 2003; Nasri et al., 2007]. These methods involve RT-PCR coupled with sequencing of the amplified product to identify the "molecular serotype" of the virus. Methods based on the VP1 gene region in particular have been shown to provide serotype identification that is comparable to standard neutralization tests [Oberste et al., 1999]. Although the majority of these methods have been designed to work on viral isolates, methods that utilize primary clinical specimens have also been described [Casas et al., 2001; Nix et al., 2006]. During large outbreaks of HFMD, the ability to determine the human enterovirus serotype quickly and efficiently in a cost effective manner would definitely contribute towards decisions on public health intervention and management. In this study, the accuracy of sequencing three separate gene regions of the enterovirus genome (VP4, VP2, and VP1) for typing enterovirus isolates of HEV-A, HEV-B, and HEV-C was compared. Three separate published RT-PCR protocols [Ishiko et al., 2002; Oberste et al., 2003; Nasri et al., 2007] that target all three gene regions of interest were used. Sequences generated from these gene regions were then compared to each other, using the VP1 gene region as a reference, in its ability to type HEV-A, HEV-B, and HEV-C viruses.

MATERIALS AND METHODS

Virus Isolation

Human enterovirus isolates from Sarawak used in this study were cultured during the course of several surveillance programs run by this laboratory in collaboration with the Sarawak Health Department over a 10-year period (1998–2008). South Vietnamese human enetrovirus isolates were obtained through collaboration within the Asia-Pacific Enterovirus Surveillance Network (APNET, http://www.apnet.org.au/) formed in 1999. All human enteroviruses were propagated in human rhabdomyosarcoma (RD) or human embryonic kidney (293) cell lines.

RNA Extraction

Viral nucleic acids were extracted from all culture harvests using the High Pure Viral Nucleic Acid Kit (Roche Diagnostics, Manheim, Germany) according to instructions provided by the manufacturer. Typically, extraction was done from 200 µl of culture harvest, eluted in 50 µl of sterile ultra high quality RNase-free water and stored at −80°C until use.

RT-PCR for HEV Identification

The presence of human enterovirus RNA was determined using a previously published pan-HEV RT-PCR method [Romero and Rotbart, 1993] that targets a region of the 5′UTR. Electrophoresis gel analysis was used to determine the presence of amplified human enterovirus RNA.

RT-PCR and Sequencing for HEV Typing

Three different published RT-PCR methods targeting the VP4 [Ishiko et al., 2002], VP2 [Nasri et al., 2007], and VP1 [Oberste et al., 2003] gene regions were used for human enterovirus typing. Each RT-PCR method was performed according to conditions published by the respective authors. All amplicons were analyzed by agarose gel electrophoresis. Amplicons were purified from the gel using the GENECLEAN III kit (BIO101, Vista, San Diego, CA). Purified products were sequenced in both directions using both the sense and antisense PCR primers of that method. Sequencing was done using the BigDye v3.2 (Applied Biosystems, Foster City, CA) and performed in the 3130 Genetic Analyzer (Applied Biosystems). Sequences were prepared and primer sequences removed using SeqMan software (DNASTAR, Madison, WI). The final consensus sequence for the VP4, VP2, and VP1 gene regions were 207, 368, and 357 bp, respectively.

Sequence Data Set

Sequence information for the VP4, VP2, and VP1 regions using methods described above, were generated from 72 Sarawak and 14 South Vietnam human enterovirus isolates examined in this study (Table I). Additionally, a total of 55 paired VP4 and VP1 sequences of Japanese HEV-A isolates mainly from cases with HFMD or herpangina were used [Hosoya et al., 2007]. A further 203 published paired VP4 and VP1 HEV-A sequences from Sarawak, Australia, South Korea, South Vietnam, Peninsular Malaysia, Saudi Arabia, Thailand, China, and United Kingdom [McMinn et al., 2001; Cardosa et al., 2003; Li et al., 2005; Simmonds and Welch, 2006; Perera et al., 2007; Tu et al., 2007] were obtained from GenBank and also evaluated.

Sequence Analysis and Phylogenetic Relationships

To determine the human enterovirus type, sequences of the three different gene regions were aligned separately. Each alignment included the corresponding sequence of each human enterovirus prototype strain obtained from GenBank. Alignments were performed using the MegAlign software (DNASTAR) which was also used to generate the nucleotide identity scores (percent of nucleotide homology) of each query sequence compared to the human enterovirus prototype sequences. As proposed by Oberste et al. [2003], if the highest score was >75% and the next highest score was <70%, then the sequence would be assigned the same serotype identity as the prototype human enterovirus paired to the highest score. However, if the highest score was between 70% and 75%, then the sequence was assigned a preliminary serotype identity of the matching prototype human enterovirus pending more sensitive typing methods.

Separate phylogenetic trees for the VP4, VP2, and VP1 gene regions were prepared using the *MEGA*

TABLE I. A Comparison of Three Different Gene Regions to Type Human Enterovirus (HEV) Isolates by Using the Nucleotide Identity Score

	VP4[a]		VP2[b]		VP1		
Isolate	Type	Highest % nucleotide identity	Type	Highest % nucleotide identity	Type	Highest % nucleotide identity	HEV species[c]
SB1806	HEV71	82.1	HEV71	80.4	HEV71	82.3	A
SB1988	HEV71	82.6	HEV71	79.7	HEV71	80.7	A
SB2278	HEV71	81.6	HEV71	80.8	HEV71	82.7	A
SB10280	HEV71	80.7	HEV71	80.8	HEV71	81.7	A
SB12682	HEV71	83.1	HEV71	82.9	HEV71	83.7	A
MY104-9	HEV71	82.1	HEV71	80.1	HEV71	84.0	A
SB64543	HEV71	82.6	HEV71	81.1	HEV71	84.0	A
VN51192	HEV71	80.2	HEV71	80.8	HEV71	83.7	A
VN5540	HEV71	83.1	HEV71	81.1	HEV71	86.0	A
VN5707	HEV71	82.1	HEV71	82.5	HEV71	83.3	A
VN5718	HEV71	82.1	HEV71	82.5	HEV71	82.3	A
VN5730	HEV71	82.6	HEV71	79.4	HEV71	82.3	A
VN5776	HEV71	80.7	HEV71	80.4	HEV71	83.7	A
VN5777	HEV71	81.6	HEV71	79.4	HEV71	82.3	A
VN5925	HEV71	80.2	HEV71	79.7	HEV71	85.3	A
VN5933	HEV71	80.7	HEV71	80.8	HEV71	82.7	A
SB2001	CVA16	81.2	CVA16	74.8	CVA16	78.3	A
S1283	CVA16	80.7	CVA16	75.5	CVA16	78.7	A
VN5607	CVA16	81.2	CVA16	76.2	CVA16	78.7	A
S114351	CVA14	84.1	CVA14	85.3	CVA14	84.7	A
SB65972	CVA12	76.8	CVA12	78.9	CVA12	81.8	A
SB4000	CVA10	80.7	CVA10	74.7	CVA10	79.1	A
SB12012	CVA10	78.3	CVA10	73.7	CVA10	76.8	A
SB12326	CVA10	76.3	CVA10	73.7	CVA10	76.8	A
SB13031	CVA10	76.3	CVA10	73.7	CVA10	76.8	A
CNS31323	CVA10	76.3	CVA10	74.0	CVA10	77.4	A
SB67851	CVA8	85.0	CVA8	82.4	CVA8	85.0	A
SB12030	CVA6	79.2	CVA6	81.5	CVA6	84.2	A
VN5710	CVA6	77.8	CVA6	81.5	CVA6	84.5	A
SB10052	CVA5	79.7	NS	—	CVA5	83.5	A
SB64742	CVA5	84.1	CVA5	82.7	CVA5	84.2	A
SB11605	CVA4	88.9	CVA4	88.4	CVA4	85.9	A
SB13128	CVA4	86.0	CVA4	84.2	CVA4	86.9	A
SB610474	CVA3	75.8	CVA3	76.1	CVA3	75.9	A
SB7470	CVA2	78.3	CVA2	80.6	CVA2	80.1	A
S17271	CVA2	78.3	CVA2	81.0	CVA2	80.1	A
CNS32573	E1,HEV75	84.5	E1	80.1	E1	79.4	B
CNS613151	CVB4	83.1	NA	—	E1	79.4	B
SB11993	E20	82.1	E3	77.2	E3	81.9	B
SB13332	E20	81.2	E3	77.2	E3	81.9	B
CNS34292	E20	82.6	E3	77.2	E3	81.6	B
CNS34293	E20	82.6	E3	77.9	E3	81.6	B
SB2598	E5	82.6	E5	81.0	E5	81.5	B
SB2640	E5	83.1	E5	80.3	E5	81.8	B
SB12804	E6	82.1	E6	78.8	E6	74.7	B
D94S1	E7	82.1	E6	78.2	E6	76.2	B
SB6067	E6,7,17;HEV75	83.1	E7	78.5	E7	78.8	B
SB15056	HEV75	83.6	E7	76.9	E7	79.4	B
VN51140	CVB3	83.1	E7	78.8	E7	81.6	B
SB12978	E29	81.2	E9	82.6	E9	84.7	B
VN5773	E32	82.6	NA	—	E9	86.9	B
SB611217	CVB1	86.5	E12	80.8	E12	81.9	B
SB9352	E4	78.7	E14	77.7	E14	75.3	B
B132S2	E15	79.7	E15	78.1	E15	78.7	B
SB7629	E16	83.6	E16	76.1	E16	80.6	B
CNS996392	E19	86.5	E19	80.1	E19	79.6	B
B11S2	E12,20	85.5	E19	78.5	E19	80.2	B
SB600724	E12,20	85.5	E19	79.2	E19	80.6	B
CNS21263	CVB4,E20	83.1	E20	80.1	E20	80.4	B
SB13652	E27	81.6	E27	84.0	E27	85.5	B
CNS21593	E19	82.6	E29	77.9	E29	78.8	B
SB14374	CVB3,4;E24	79.2	E30	79.8	E30	80.9	B
SB14486	CVB4	82.6	E30	81.1	E30	80.9	B

(*Continued*)

TABLE I. (*Continued*)

Isolate	VP4[a] Type	VP4[a] Highest % nucleotide identity	VP2[b] Type	VP2[b] Highest % nucleotide identity	VP1 Type	VP1 Highest % nucleotide identity	HEV species[c]
SB11373	E19	84.1	E33	77.9	E33	78.5	B
CNS3583	E19	84.1	E33	77.9	E33	78.8	B
SB10405	E19	83.6	CVB2	81.6	CVB2	82.1	B
SB10406	E19	83.6	CVB2	81.6	CVB2	82.1	B
SB12296	E19	84.1	CVB2	82.0	CVB2	81.8	B
SB13078	E19	84.1	CVB2	81.6	CVB2	81.2	B
CNS22473	E32	83.6	CVB2	81.6	CVB2	81.8	B
VN5555	HEV75	82.6	NS	—	CVB2	84.9	B
SB12597	E7	81.2	CVB3	78.9	CVB3	74.7	B
D29S1	CVB4	84.1	CVB4	82.4	CVB4	81.0	B
SB3951	CVB1	85.5	CVB5	81.8	CVB5	81.8	B
SB18674	CVB2	83.1	CVA9	80.1	CVA9	81.0	B
SB6376	E20	82.6	NS	—	HEV73	76.9	B
B105S1	CVA13	81.6	NS	—	CVA13	72.4	C
SB1220	CVA11	81.6	CVA17	77.7	CVA17	78.0	C
SB1543	CVA11	81.6	NA	—	CVA17	78.0	C
SB7508	CVA21	90.8	CVA21	87.6	CVA21	89.4	C
CNS20514	CVA21	90.3	CVA21	90.3	CVA21	90.0	C
SB7293	CVA24	83.6	CVA24	84.8	CVA24	85.0	C
SB8403	CVA24	84.1	CVA24	84.8	CVA24	85.0	C
CNS30014	CVA11	83.1	CVA24	72.6	CVA24	71.3	C
CNS51093	CVA24	84.1	CVA24	85.1	CVA24	84.7	C
CNS51214	CVA24	84.1	CVA24	84.4	CVA24	85.3	C

[a]Nucleotide identity scores >75% to multiple serotypes was observed.
[b]NA, no amplification by RT-PCR; NS, no sequence obtained after multiple attempts to sequence from either strand.
[c]Classification done according to VP1 data.

version 4, available at http://www.megasoftware.net [Tamura et al., 2007]. Neighbor-joining (NJ) phylogenetic trees were generated using a maximum composite likelihood model of nucleotide substitution. The statistical significance of the phylogenies constructed was estimated by bootstrap analysis using 1,000 pseudo-replicate data sets.

RESULTS

Performance of the Different RT-PCR Methods

A total of 86 different human enterovirus isolates comprising those from Sarawak and South Vietnam were included in this study. The presence of human enterovirus RNA in all nucleic acid extracts from these isolates was confirmed by a pan-human enterovirus RT-PCR method that targets the 5'UTR region [Romero and Rotbart, 1993]. Extracts from all 86 isolates were positive for human enterovirus using this method. To type these isolates, three different RT-PCR methods that target the VP4, VP2, and VP1 gene regions, respectively, were used. Both the VP4 and VP1 methods successfully amplified all 86 isolates tested and sequence data were obtained from all amplicons. However, the VP2 method failed to amplify three isolates (CNS613151, SB1543, and VN5773) (Table I). Additionally, sequence could not be obtained from amplicons generated by the VP2 method for four other isolates (SB10052, SB6376, B105S1, and VN5555) even after multiple attempts to generate sequence data from either strand (Table I).

HEV Typing

The partial VP1 sequence data (this study and all human enterovirus prototype sequences from GenBank) was used to initially prepare a bootstrapped phylogenetic tree (data not shown) to determine the species group (HEV-A to D) of all the 86 human enterovirus isolates in this study. From this analysis, a total of 36 HEV-A, 40 HEV-B, and 10 HEV-C were identified (Table I). All further analysis was done separately for each human enterovirus species group. Results were compared to typing by VP1 which was used as the reference standard.

HEV-A

Using the criteria proposed by Oberste et al. [2003] as described in the methods section, the highest nucleotide identity (HNI) score for each gene region (VP4, VP2, and VP1) was used to generate preliminary serotype identification for each of the 86 human enterovirus isolates in this study (Table I). For the 36 HEV-A isolates investigated, a 100% concordance of serotype identification by all three gene regions was observed. This was observed despite the fact that some of the HNI scores for the VP2 region were below 75% (indicating a tentative identification by that method) and all the HNI scores generated from VP4 sequences had multiple nucleotide identity scores greater than 75% to other serotypes (indicating potential inconclusive serotype identification). However, separate phylogenetic analysis of each gene region showed that in every case, HEV-A isolates

clustered (bootstrap support of >70%) with the prototype strain of the serotype determined using the HNI score (Fig. 1). Taken together, HNI scores coupled with phylogenetic analysis provide a useful way of typing HEV-A isolates using any of the three gene regions (VP4, VP2, and VP1) investigated in this study.

HEV-B

Preliminary serotype identification of HEV-B isolates using the HNI scores showed that there was a 100% concordance between the VP2 and VP1 gene regions. However, only seven isolates (17.5%) typed by VP4 matched the preliminary serotype identification obtained using VP2 and VP1 (Table I). As with the HEV-A isolates, VP4 sequences showed multiple HNI scores >75% to other serotypes. In addition, identical HNI scores to more than one serotype (for isolates CNS32573, SB6067, B11S2, SB600724, CNS21263, and SB14374) were observed with VP4. It was also observed that for VP4, serotype identification with HNI scores generally did not match clustering to the same prototype strain in the phylogenetic tree (Fig. 2). For example, isolates SB11993, SB13332, CNS34292, and CNS34293 had HNI scores >75% to E20 but clustered together with E3 in the phylogenetic tree (Fig. 2). On the contrary, for both VP2 and VP1, there was a 100% match between HNI scores to, and phylogenetic clustering with, the same prototype strain for all HEV-B isolates tested. The results suggest that only the VP2 and VP1 gene regions would be useful for serotype identification of HEV-B viruses.

HEV-C

HEV-C isolates investigated in this study also showed a 100% concordance between the VP2 and VP1 data for serotype identification using the HNI scores (Table I). With the exception of two isolates (B105S1 and CNS30014), there was a correlation between serotype identification with HNI scores and phylogenetic clustering (Fig. 3) to the same prototype strain using either of these gene regions. However, for isolates B105S1 (for VP1 only; no sequence was obtained from VP2) and CNS30014 (for both VP1 and VP2), with HNI scores between 70% and 75% to CVA13 and CVA24,

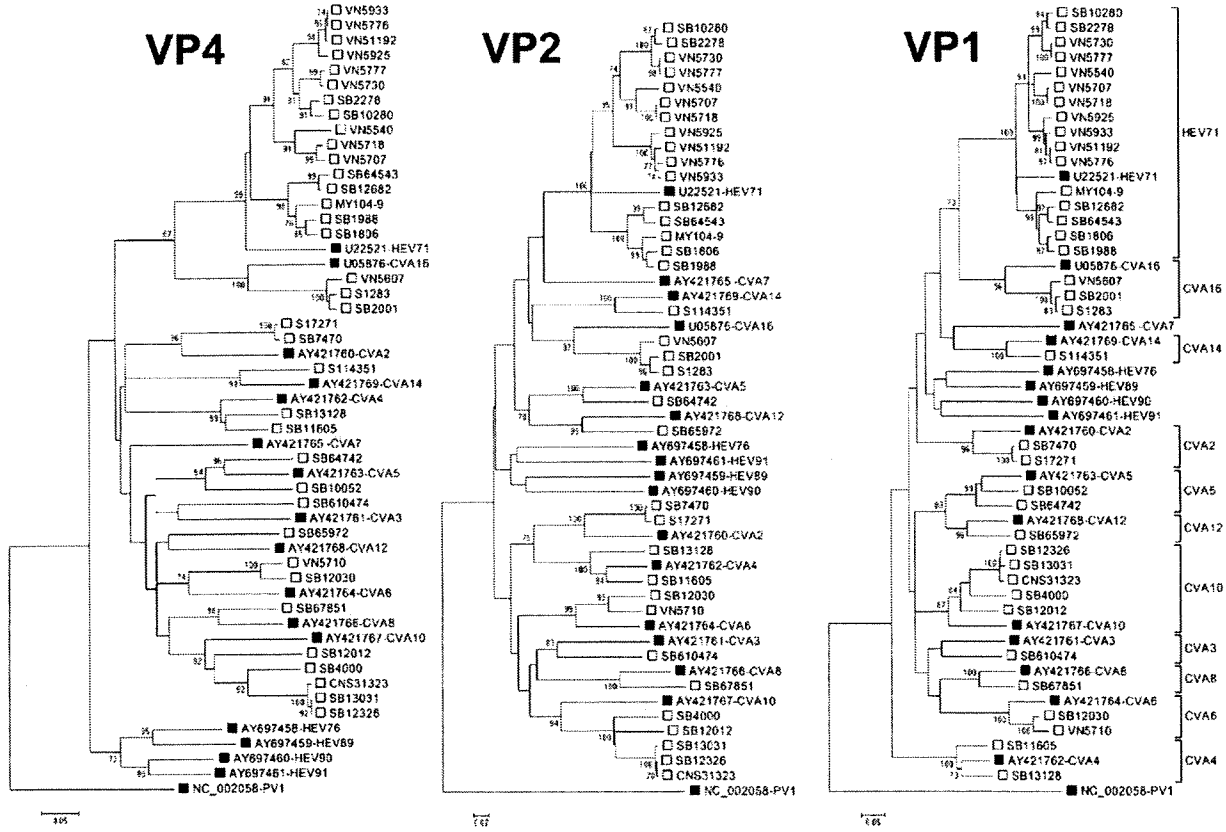

Fig. 1. Phylogenetic trees showing the relationships of HEV-A isolates based on the VP4, VP2, and VP1 gene regions. All trees include the HEV-A isolates listed in Table I (open boxes) and prototype sequences obtained from GenBank (closed boxes). Trees are rooted using PV1 (GenBank accession no. NC_002058), all horizontal branch lengths are drawn to a scale of nucleotide substitutions per site, and bootstrap value >70% are indicated at key nodes. All the different serotypes identified from the study set using VP1 are indicated to right of the VP1 tree.

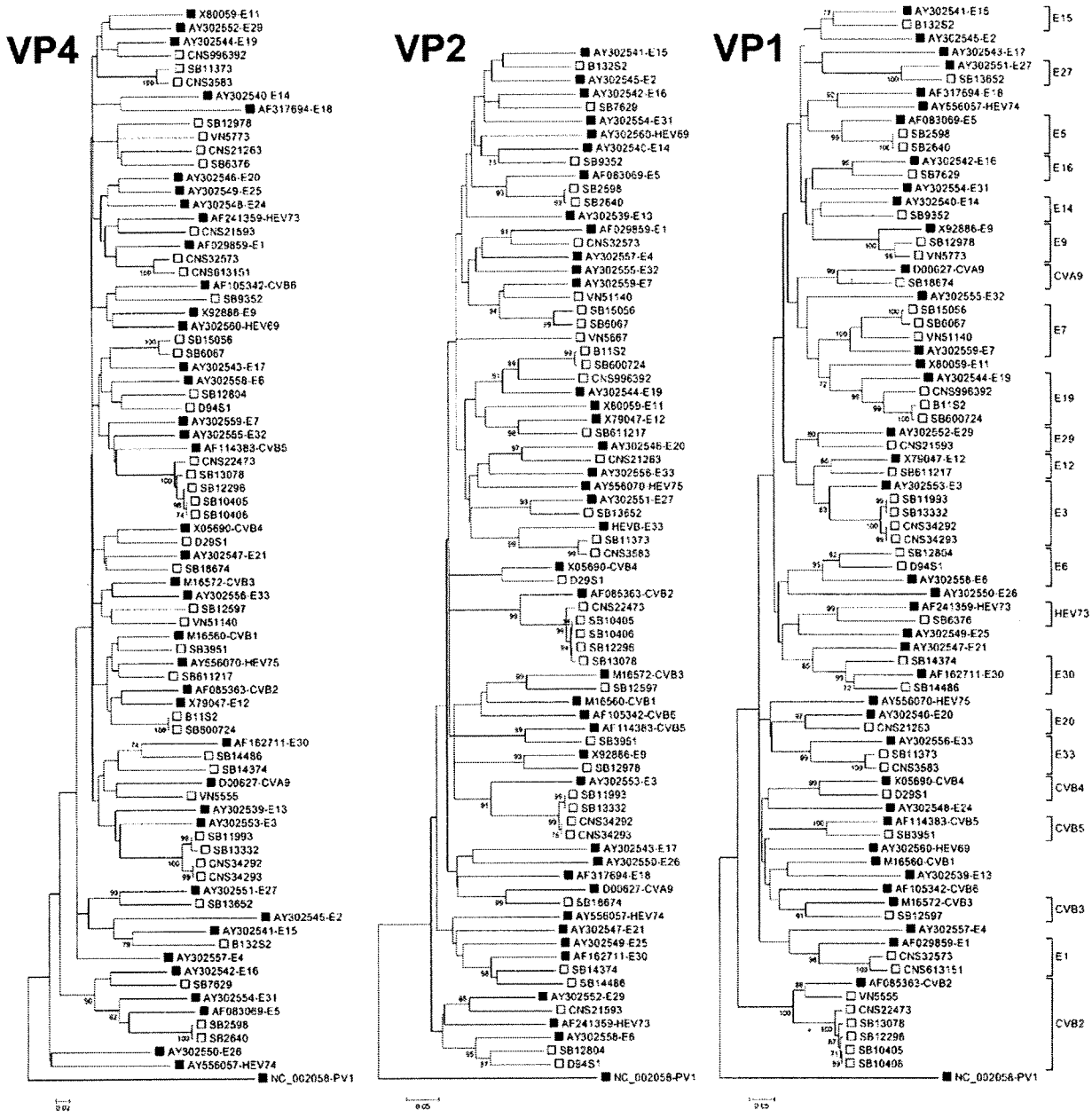

Fig. 2. Phylogenetic trees showing the relationships of HEV-B isolates based on the VP4, VP2, and VP1 gene regions. All trees include the HEV-B isolates listed in Table I (open boxes) and prototype sequences obtained from GenBank (closed boxes). Trees are rooted using PV1 (GenBank accession no. NC_002058), all horizontal branch lengths are drawn to a scale of nucleotide substitutions per site, and bootstrap value >70% are indicated at key nodes. All the different serotypes identified from the study set using VP1 are indicated to right of the VP1 tree.

respectively, clustering to the same prototype strain in the phylogenetic tree did not occur (Fig. 3). As such, using the definition proposed by Oberste et al. [2003], serotype identification of both these isolates remains tentative pending more sensitive identification methods. When using VP4, there was a 70% concordance of serotype identification by HNI scores when compared to VP1. However, as observed with HEV-B isolates, VP4 HNI scores to a particular serotype did necessarily mean clustering to the same prototype strain in the phylogenetic tree. For example, isolate CNS30014 had a VP4 HNI score of 83.1% to CVA11 (Table I) but clustered with CVA20 in the phylogenetic tree (Fig. 3). Even when there was a match between VP4 HNI identification and clustering to the same prototype strain in the phylogenetic tree, a potential misassignment of the

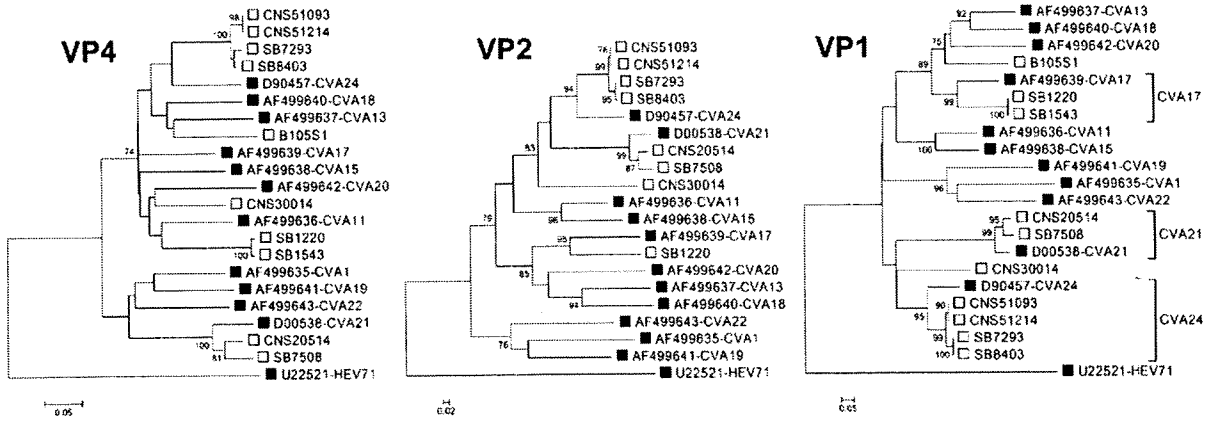

Fig. 3. Phylogenetic trees showing the relationships of HEV-C isolates based on the VP4, VP2, and VP1 gene regions. All trees include the HEV-C isolates listed in Table I (open boxes) and prototype sequences obtained from GenBank (closed boxes). Trees are rooted using HEV71 (GenBank accession no. U22521), all horizontal branch lengths are drawn to a scale of nucleotide substitutions per site, and bootstrap value >70% are indicated at key nodes. All the different serotypes identified from the study set using VP1 are indicated to right of the VP1 tree.

serotype identity may occur. For example, isolates SB1220 and SB1543 typed as CVA11 by VP4 were identified as CVA17 by VP1 (Table I). Taken together, only the VP2 and VP1 gene regions are useful for serotype identification of HEV-C viruses.

Typing of Additional HEV-A Viruses

Since the data showed that VP4 could be used to accurately assign serotype to HEV-A viruses, it was decided to investigate if this observation holds true using data obtained by other laboratories. VP2 was not included in this part of the analysis because there is very little published data of paired VP4 and VP2 sequences. A total of 55 Japanese and 203 published paired VP4 and VP1 sequences comprising eight different serotypes of HEV-A (HEV71, CVA2, CVA4, CVA5, CVA6, CVA10, CVA12, and CVA16) were analyzed in the same way as described above (data not shown). There was a 100% concordance of serotype identification by using the HNI scores of either VP4 or VP1. Additionally, all serotypes identified by HNI scores of either VP4 or VP1 correctly clustered with their prototype strain in the phylogenetic analysis (data not shown), thus confirming that indeed VP4 sequence can assign reliably serotype to HEV-A strains.

DISCUSSION

In recent years, molecular typing methods have been reported as useful and rapid tools for typing human enteroviruses [Casas et al., 2001; Ishiko et al., 2002; Oberste et al., 2003; Nasri et al., 2007]. Most of these methods have targeted the virus capsid protein coding regions. Of these methods, the sequencing of a portion of the VP1 capsid protein coding region has been widely used by several laboratories as a means for human enterovirus identification [Oberste et al., 2003; Blomqvist et al., 2008]. The VP1 nucleotide sequence has been shown to provide human enterovirus typing identification that correlates to neutralization tests [Oberste et al., 1999]. However, little has been done to compare directly other protein coding regions to VP1 in identification of human enteroviruses although methods using other regions have separately been published. In this study the usefulness of the complete VP4 and partial VP2 gene regions in human enterovirus typing using a partial VP1 nucleotide region as a reference standard was investigated. This results have shown that the percentage of nucleotide homology to prototype sequences (HNI scores) coupled with phylogenetic analysis provide a useful way to type human enteroviruses. Altogether, this study has shown that typing by VP1 or VP2 would be useful for HEV-A, HEV-B, and HEV-C viruses, confirming results obtained by others [Nasri et al., 2007] whereas typing using VP4 would be useful only for assigning serotype to HEV-A viruses.

The high rate of mutation [Takeda et al., 1994; Brown et al., 1999; Martin et al., 2000] observed for human enteroviruses could potentially lead to newer strains with sufficient mutations that could affect the performance of primers used in RT-PCR-based typing methods. Thus, the ability to use more than one method or gene region to type HEV would certainly enhance the capability of a laboratory to type these viruses. As an example, in this study, it has been observed that the partial VP2 primer set failed to amplify or sequence some viruses of HEV-A, HEV-B, and HEV-C which was successfully amplified by both the VP4 and VP1 methods. Similar observations have also been reported by others in which recent human enterovirus strains have been typed successfully using the VP2 method but failed to be amplified using the VP1 method [Nasri et al., 2007]. Interestingly, in the study by Nasri et al. [2007], four of the viruses that failed to be amplified by the VP1 method were typed as HEV71 (HEV-A) using the VP2

method. Based on the results of this study, these HEV71 viruses could potentially have been typed by the VP4 method to confirm the typing results obtained with the VP2 method.

The sequences obtained from these typing methods could also be useful for epidemiological studies that track evolution, migration, and emergence of HEV. For example, in reported studies of HFMD, for two of the major causative agents (HEV71 and CVA16), genotyping using the VP4 sequence has been shown to correlate with the genotype profile obtained using complete VP1 sequence [Cardosa et al., 2003; Perera et al., 2007]. Generating a shorter PCR amplicon (207 bp for VP4 vs. 891 bp for VP1 for both HEV71 and CVA16), the VP4 gene region is useful as a rapid screening tool to determine genotype profiles of theses viruses during large outbreaks of HFMD [Hosoya et al., 2007]. This information can then be used for informed decisions on which isolates to sequence for the complete VP1 as a way to improve efficiency and cost when dealing with very large numbers of isolates. In addition, sequencing for the VP4 gene region reduces cost as only a single sequencing reaction of one strand of the amplicon is sufficient to generate complete VP4 sequence as the primer binding sites are located outside of the target region (in 5′UTR and VP2). In contrast, the published method for molecular typing using the partial VP1 gene region requires two sequencing reactions targeting both strands of the amplicon to generate the partial VP1 sequence as the primer binding sites are immediately flanking the target region.

In conclusion, it is proposed that typing for HEV-A, HEV-B, and HEV-C can be achieved using either the partial VP1 or VP2 method or a combination of both if one fails to amplify or generate sequence of a particular isolate. In addition, any of the three methods evaluated would be useful for typing HEV-A viruses. Therefore, in large HFMD outbreaks where the predominant causative agents are HEV-A viruses, the VP4 method offers not only cost-saving measures to the laboratory but additionally the VP4 sequence itself offers a rapid way to provide information about the genotype of the virus in the case of HEV71 and CVA16. These options for typing human enteroviruses would certainly help in enhancing the capability of any laboratory working with these viruses.

ACKNOWLEDGMENTS

We thank collaborators in Vietnam and Japan for sharing their sequences used in this study.

REFERENCES

Ang LW, Koh BK, Chan KP, Chua LT, James L, Goh KT. 2009. Epidemiology and control of hand, foot and mouth disease in Singapore, 2001–2007. Ann Acad Med Singapore 38:106–112.

Blomqvist S, Paananen A, Savolainen-Kopra C, Hovi T, Roivainen M. 2008. Eight years of experience with molecular identification of human enteroviruses. J Clin Microbiol 46:2410–2413.

Brown BA, Oberste MS, Alexander JP, Kennett MLJ, Pallansch MA. 1999. Molecular epidemiology and evolution of enterovirus 71 strains isolated from 1970 to 1998. J Virol 73:9969–9975.

Cardosa MJ, Perera D, Brown BA, Cheon D, Chan HM, Chan KP, Cho H, McMinn PC. 2003. Molecular epidemiology of human enterovirus 71 strains and recent outbreaks in the Asia-Pacific region: Comparative analysis of the VP1 and VP4 genes. Emerg Infect Dis 9:461–468.

Casas I, Palacios GF, Trallero G, Cisterna D, Freire MC, Tenorio A. 2001. Molecular characterization of human enteroviruses in clinical samples: Comparison between VP2, VP1, and RNA polymerase regions using RT nested PCR assays and direct sequencing of products. J Med Virol 65:138–148.

Hosoya M, Kawasaki Y, Sato M, Honzumi K, Hayashi A, Hiroshima T, Ishiko H, Kato K, Suzuki H. 2007. Genetic diversity of coxsackievirus A16 associated with hand, foot, and mouth disease epidemics in Japan from 1983 to 2003. J Clin Microbiol 45:112–120.

Ishiko H, Shimada Y, Yonaha M, Hashimoto O, Hayashi A, Sakae K, Takeda N. 2002. Molecular diagnosis of human enteroviruses by phylogeny-based classification by use of the VP4 sequence. J Infect Dis 185:744–754.

Li L, He Y, Yang H, Zhu J, Xu X, Dong J, Zhu Y, Jin Q. 2005. Genetic characteristics of human enterovirus 71 and coxsackievirus A16 circulating from 1999 to 2004 in Shenzhen, People's Republic of China. J Clin Microbiol 43:3835–3839.

Lin TY, Twu SJ, Ho MS, Chang LY, Lee CY. 2003. Enterovirus 71 outbreaks, Taiwan: Occurrence and recognition. Emerg Infect Dis 9:291–293.

Martin J, Dunn G, Hull R, Patel V, Minor PD. 2000. Evolution of the Sabin strain of type 3 poliovirus in an immunodeficient patient during the entire 637-day period of virus excretion. J Virol 74:3001–3010.

McMinn PC. 2002. An overview of the evolution of enterovirus 71 and its clinical and public health significance. FEMS Microbiol Rev 26:91–107.

McMinn PC, Lindsay K, Perera D, Chan HM, Chan KP, Cardosa MJ. 2001. Phylogenetic analysis of enterovirus 71 strains isolated during linked epidemics in Malaysia, Singapore, and Western Australia. J Virol 75:7732–7738.

Miyazawa I, Azegami Y, Kasuo S, Yoshida T, Kobayashi M, Shiraishi T. 2008. Prevalence of enterovirus from patients with herpangina and hand, foot and mouth disease in Nagano Prefecture, Japan, 2007. Jpn J Infect Dis 61:247–248.

Nasri D, Bouslama L, Omar S, Saoudin H, Bourlet T, Aouni M, Pozzetto B, Pillet S. 2007. Typing of human enterovirus by partial sequencing of VP2. J Clin Microbiol 45:2370–2379.

Nix WA, Oberste MS, Pallansch MA. 2006. Sensitive, seminested PCR amplification of VP1 sequences for direct identification of all enterovirus serotypes from original clinical specimens. J Clin Microbiol 44:2698–2704.

Oberste MS, Maher K, Kilpatrick DR, Pallansch MA. 1999. Molecular evolution of the human enteroviruses: Correlation of serotype with VP1 sequence and application to picornavirus classification. J Virol 73:1941–1948.

Oberste MS, William AN, Maher K, Pallansch MA. 2003. Improved molecular identification of enteroviruses by RT-PCR and amplicon sequencing. J Clin Virol 26:375–377.

Perera D, Yusof MA, Podin Y, Ooi MH, Thao NT, Wong KK, Zaki A, Chua KB, Malik YA, Tu PV, Tien NT, Puthavathana P, McMinn PC, Cardosa MJ. 2007. Molecular phylogeny of modern coxsackievirus A16. Arch Virol 152:1201–1208.

Podin Y, Gias ELM, Ong F, Leong Y-W, Yee S-F, Yusof MA, Perera D, Teo B, Wee T-Y, Yao S-C, Yao S-K, Kiyu A, Arif MT, Cardosa MJ. 2006. Sentinel surveillance for human enterovirus 71 in Sarawak, Malaysia: Lessons from the first 7 years. BMC Public Health 6:180.

Romero JR, Rotbart HA. 1993. PCR detection of the human enteroviruses. In: Persing DH, Smith TF, Tenover FC, White TJ, editors. Diagnostic molecular microbiology: Principles and applications. Washington DC: American Society for Microbiology. pp 401–406.

Simmonds P, Welch J. 2006. Frequency and dynamics of recombination within different species of human enteroviruses. J Virol 80:483–493.

Stanway G, Brown F, Christian P, Hovi T, Hypia T, King AMQ, Knowles NJ, Lemon SM, Minor PD, Pallansch MA, Palmenberg AC, Skern T. 2005. Family *Picornaviridae*. In: Fauquet CM, Mayo MA, Maniloff J, Desselberger U, Ball LA, editors. Virus taxonomy: Eight report of the International Committee on Taxonomy of Viruses. United Kingdom: Elsevier/Academic Press. pp 757–778.

Takeda N, Tanimura M, Miyamura K. 1994. Molecular evolution of the major capsid protein VP1 of enterovirus 70. J Virol 68:854–862.

Tamura K, Dudley J, Nei M, Kumar S. 2007. MEGA4: Molecular evolutionary genetics analysis (MEGA) software version 4.0. Mol Biol and Evol 24:1596–1599.

Tu PV, Thao NT, Perera D, Huu TK, Tien NT, Thuong TC, How OM, Cardosa MJ, McMinn PC. 2007. Epidemiologic and virologic investigation of hand, foot, and mouth disease, southern Vietnam, 2005. Emerg Infect Dis 13:1733–1741.

Yamashita T, Ito M, Taniguchi A, Sakae K. 2005. Prevalence of coxsackievirus A5, A6, and A10 in patients with herpangina in Aichi Prefecture, 2005. Jpn J Infect Dis 58:390–391.

Zhang Y, Tan XJ, Wang HY, Yan DM, Zhu SL, Wang DY, Ji F, Wang XJ, Gao YJ, Chen L, An HQ, Li DX, Wang SW, Xu AQ, Wang ZJ, Xu WB. 2009. An outbreak of hand, foot, and mouth disease associated with subgenotype C4 of human enterovirus 71 in Shandong, China. J Clin Virol 44:262–267.